

Sound wave attenuation in a duct with a periodic array of ultrathin Helmholtz resonators

Cédric Maury

Ecole Centrale Marseille, Laboratoire de Mécanique et d'Acoustique (LMA), UPR-CNRS 7051, Aix Marseille Université, 38 rue Frédéric Joliot-Curie, 13013 Marseille, France.

Teresa Bravo

Instituto de Tecnologías Físicas y de la Información (ITEFI), Consejo Superior de Investigaciones Científicas (CSIC), Serrano 144, 28006 Madrid, Spain.

Summary

Enhancing the broadband attenuation of low-frequency noise using compact, lightweight and fiber-free acoustic liners is still a challenging task in air conditioning systems, but also in exhaust and intake ducted flows. Locally-reacting Helmholtz resonators can be tuned and optimized to efficiently dissipate noise in a narrow mid-frequency range. A periodic combination of several resonators is known to provide a broader bandwidth of the noise attenuated at mid-frequencies, albeit at constant value of the total power over the attenuation bandwidth. In this work, a theoretical study examines the efficiency of a periodic array of Ultrathin Helmholtz Resonators (UHR) to attenuate low-frequency noise components over a broad bandwidth, well below the first cut-on frequencies of the duct and of the resonators neck and cavity. Each side-branch resonator is composed of a cylindrical neck backed by a coplanar coiled air chamber that significantly increases the acoustic path length in the cavity while keeping a sub-wavelength depth of the cavity at the resonator Helmholtz resonance. A transfer matrix formulation is derived to calculate the Transmission Loss (TL) of the array of resonators, averaged over the number of resonators. The TL results tend towards the dispersion curves of the unitary transfer matrix as the number of resonators increases, revealing the emergence of stopping and passing bands that respectively inhibit and allow the propagation of sound waves in the duct. The attenuation characteristics of the array of UHRs are compared to that due to arrays of classical Helmholtz resonators in the no-flow and uniform flow cases. Of interest is to find an optimal periodic distance between the resonators, typically half the acoustic wavelength at the Helmholtz resonance, in order to broaden the bandwidth of the first stop-band in the low-frequency range.

PACS no. 43.50.Gf, 43.20.Mv

1. Introduction

The difficulty in the design of acoustic absorbers, being both efficient in the low frequency range while maintaining a reasonable size as a linear dissipative system, is an open problem subjected to current research. The classical Helmholtz Resonator (HR) constitutes a standard noise control device that provides good absorption values, but confined within a narrow frequency band [1]. To enhance their acoustical performance, different types of resonator combinations can be used. This is the physical approach considered for a locally-reacting partition composed of single or multiple layers of perforated or micro-perforated panels backed by a cavity filled with honeycomb material and undergoing plane wave forcing. High

absorption is achieved by energy dissipation from the viscous friction forces on the perforation holes when the acoustic boundary layer is of comparable thickness to the holes radius at the resonance frequency of the backing cavity.

In ducts, attenuating the propagation of plane waves at low frequency finds applications in noise mitigation of air conditioning systems in buildings as well as in surface and air transport domains. For instance, an array of dissimilar HRs has been considered by Trochidis [2] as an alternative to the conventional types of dissipative mufflers under plane wave propagation condition. The effect of several parameters on the Transmission Loss (TL) was studied, including the position of the longer and shorter resonator elements as well as the length of their openings for a given combination of

elements. A slightly different approach has been proposed by Bradley [3] that considered a periodic waveguide filled with a viscous and heat-conducting fluid under a time harmonic excitation. The duct was composed of localized scattering sections connected by lengths of uniform waveguides. It was shown that this system can be described by forward and backward travelling Bloch wave functions, leading to various propagation features linked to axial standing waves and scatterer's resonances. A similar analysis has been pursued and applied to the attenuation of sound propagating in a train tunnel by means of a periodic array of HRs to avoid the formation of shock waves [4]. Special attention has been paid to the wave dispersion characteristics due to wall friction and to the thermoviscous diffusivity of sound. The authors explained the emergence of "stopping bands" that selectively inhibit the propagation of sound waves, and "passing bands" over which the sound waves propagate, but exhibit dispersion due to the periodic arrangement of resonators. In particular, when the axial spacing between the neighboring resonators becomes multiple of a half wavelength of sound waves, Bragg reflection occurs, hence blocking the forward transmission of sound. The sound waves then become evanescent and are rapidly damped so that they cannot propagate further away. When the frequency due to the side branch Helmholtz resonance coincides with that due to the Bragg reflection, the bandwidth of attenuation is significantly widened.

Wang and Mak [5] have built their model upon this description to study a periodic combination of side-branch resonators mounted in a one-dimensional duct without flow. They have combined Bloch wave theory with the transfer matrix method and focused on sound attenuation at low to medium frequencies, positioning the nearby resonators at a distance much larger than the neck diameter of each individual device. The analytical model has been successfully compared against a three-dimensional finite element model and against measurements performed on an experimental setup consisting of a duct with five identical side branch resonators and a loudspeaker mounted on one side and two-loads on the other side. The results showed an averaged TL between 3-15 dB extending below 600 Hz over a broader frequency range than that of a single resonator.

Although these works show promising results, the required dimensions of the resonators becomes

prohibitively large for real-life problems when one aims at progressively decreasing the frequency of maximal attenuation. In order to be able to diminish the Helmholtz resonance frequency without increasing the cavity depth, we propose in this work to coil the path followed by the acoustical wave in the cavity resonator. This is an effective way to increase the acoustic path length while constraining the required total size of the resonator. Such devices have been already investigated by Li and Assouar [6], considering a perfect acoustic absorber with deep subwavelength thickness under a normal incidence wave pressure field. Assuming a partition composed of a perforated plate with each perforation cell backed by a straight air cavity, they realized that a critical parameter governing the absorption performance value was the effective length path followed by the acoustic wave within each cell rather than the cross-sectional area of the back cavity. They showed that a coiled coplanar air chamber instead of a straight air cavity was able to provide an effective path length that significantly decreases the absorber Helmholtz resonance frequency. The normal incidence absorption spectrum predicted by their analytical model was confirmed against numerical results from a commercial finite element software. With a reduced panel-cavity thickness of only 12.2 mm, a perfect absorber has been achieved at 125.8 Hz, the Helmholtz resonance frequency of the system. This perfect absorption was however very localized around this frequency. In the present study, we propose a combination of the solutions considered in [5] and [6] to design a duct noise control device that presents good attenuation properties at low frequencies and over a broad frequency range. We aim at combining the previous solutions, *e.g.* coiled up back space in the partition to increase the effective path length and decrease the Helmholtz frequency in conjunction with a periodic array of Helmholtz resonators to create stop- and pass-bands to enhance the attenuation over a broad bandwidth.

The paper is organised as follows: in Sec. 2, we expose an analytical model that estimates the TL of a periodic array of HRs in the low- to mid-frequency range. This model is compared against published results present in the literature. A parametric study is performed in Sec. 3 on the attenuation spectra to extract the main physical constitutive parameters that need to be selected for the design of optimal HR arrays depending on the particular cost function to be fulfilled. This study

is expected to bring insights into the physical mechanisms governing the existence of stop- and pass-bands. Finally, the main conclusions and perspectives will be summarised at the end of the work.

2. Analytical model

In this section, we briefly present the analytical propagation model that corresponds to the physical arrangement shown in Fig. 1. We sequentially model the main physical components by increasing degree of complexity, considering first a single HR and then a periodic structure composed of a straight duct with coupled side-branch HRs. Each HR is then assumed to be backed by a coiled air chamber rather than by a straight air cavity. Characteristic wave types are then calculated.

2.1. Helmholtz resonator input impedance

The input impedance Z_b at the HR neck can be written in terms of the pressure p_1 and velocity v_1 at the neck entrance as

$$Z_b = \frac{p_1}{v_1} = Z_{p1} - j \frac{S_1}{S_p} Z_0 \cot(k_0 D_1), \quad (1)$$

where S_1 and S_p are respectively the cross-sections of the neck and of the backing cavity of depth D_1 . The first term is the resonator neck transfer impedance that can be described by the model of Maa [7] for a single hole of diameter d_1 and thickness t_1 as follows

$$Z_{p1} = j\omega\rho_0 t_1 \left[1 - \frac{2}{k_1 \sqrt{-j}} \frac{J_1(k_1 \sqrt{-j})}{J_0(k_1 \sqrt{-j})} \right]^{-1} + \text{cor} \sqrt{2\eta} \frac{k_1}{d_1} + j0.85\omega\rho_0 d_1, \quad (2)$$

with $\eta = 1.798 \cdot 10^{-5} \text{ kg m}^{-1} \text{ s}^{-1}$, the dynamic viscosity of air at 20°C and $k_1 = (d_1/2)/r_{\text{visc.}}(\omega)$, the perforate constant defined as the ratio of the opening radius to the viscous boundary layer thickness, $r_{\text{visc.}}(\omega) = \sqrt{\eta/\rho_0\omega}$. Eq. (2) is composed of three terms: the first term takes into consideration the hole internal impedance, the second term extra damping due to the added external resistance and the third reactance term considers the added mass external correction. According to [8], $\text{cor} = 8$ is assumed for a sharp-edged hole.

2.2. Periodic array of HRs

The single HR described in Sec. 2.1. is taken here as the base piece to build a periodic structure. The physical configuration is inspired by the system presented by Wang and Mak [5]. It is composed of a rigid duct of cross-section S_d with multiples side-branch resonators. The unit cell periodically repeated consists of one resonator plus an axial duct length D . One assumes that the frequency is well below the first duct, neck and cavity cut-on frequencies and only plane waves are considered.

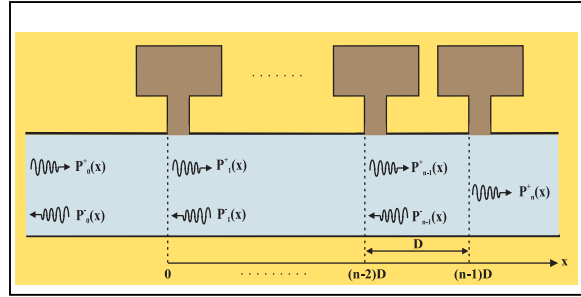


Figure 1. Sketch of a side-branch array composed of a HR unit cell periodically repeated over the duct axial length.

For each particular n^{th} unit cell, the pressure field is expressed as a combination of right-going and left-going plane waves with unknown amplitudes. We need to apply appropriate continuity conditions for the pressure and the acoustic flow rate at the interface $x = nD$ to obtain a linear 2×2 algebraic system that relates the incoming and outgoing plane wave amplitudes as

$$\begin{bmatrix} C_{n+1}^+ \\ C_{n+1}^- \end{bmatrix} = \mathbf{T} \begin{bmatrix} C_n^+ \\ C_n^- \end{bmatrix}, \quad (3)$$

with

$$\mathbf{T} = \begin{bmatrix} \left(1 - \frac{S_1 \rho_0 c_0}{2S_d Z_b}\right) e^{-ik_0 D} & -\frac{1}{2} \frac{S_1 \rho_0 c_0}{S_d Z_b} e^{ik_0 D} \\ \frac{1}{2} \frac{S_1 \rho_0 c_0}{S_d Z_b} e^{-ik_0 D} & \left(1 + \frac{S_1 \rho_0 c_0}{2S_d Z_b}\right) e^{ik_0 D} \end{bmatrix}, \quad (4)$$

the transfer matrix of the unit cell [5]. If we consider an array of N_R resonators, the total transfer matrix can be calculated as the product of the individual transfer matrices

$$\mathbf{T}_{N_R} = \prod_{i=1}^{N_R} \mathbf{T}_i = \mathbf{T}^{N_R}, \quad (5)$$

where it has been assumed that $\mathbf{T}_i = \mathbf{T}$ as the resonators are identical. In the particular case of a semi-infinite duct with an anechoic termination on the right side after the last HR (see Fig. 1), there are no waves reflected backwards so that the reflection coefficient is zero-valued and $C_{N_R}^- = 0$.

From Eq. (3), the transmitting coefficient reads

$$C_{N_R}^+ = t_{11}^{N_R} - \frac{t_{21}^{N_R}}{t_{22}^{N_R}} t_{12}^{N_R}, \quad (6)$$

and the averaged TL is given by

$$\text{TL} = \frac{20}{N_R} \log_{10} \left| \frac{C_0^+}{C_{N_R}^+} \right| = -\frac{20}{N_R} \log_{10} |C_{N_R}^+|, \quad (7)$$

assuming a unit incident plane wave, $C_0^+ = 1$.

2.3. Coiled backing cavity

In the lossless case, the input impedance of the Helmholtz resonator has been given in Sec. 2.1. by Eq. (1). For simplicity, we consider a square cavity of length (and width) a so that the neck and cavity cross-sectional areas are expressed as $S_1 = \pi d_1^2 / 4$ and $S_p = a^2$. In the coiled resonator, the cavity depth of the classic resonator D_1 is replaced by D_{1c} , the effective length path of the acoustic wave. Assuming p turns in a rectangular folded pattern with quarter-circle path at each bend, the total effective acoustic path length reads

$$D_{1c} = (2p - 1)\pi w / 2 + b + 2(p - 1)a, \quad (8)$$

provided that $2p(w + b) = a$ with w the distance between two walls and b the wall thickness.

Viscous losses may occur between the walls of the labyrinth, whose separation distance w might be less than twice the viscous boundary layer thickness $r_{\text{visc.}}(\omega)$. This adds further dissipation to the losses already accounted for by the model of Maa in the neck. The terms Z_0 and k_0 in Eq. (1) are then replaced by Z_{loss} and k_{loss}

$$Z_{\text{loss}} = Z_0 \left[1 - \frac{(1-j) C_{\text{friction}}}{\sqrt{2}} \frac{C_{\text{friction}}}{\omega/2} \sqrt{\frac{\eta}{\rho_0 \omega}} \right], \quad (9)$$

$$k_{\text{loss}} = k_0 \left[1 - \frac{(1-j) C_{\text{friction}}}{\sqrt{2}} \frac{C_{\text{friction}}}{\omega/2} \sqrt{\frac{\eta}{\rho_0 \omega}} \right], \quad (10)$$

where the friction coefficient, $C_{\text{friction}} = 1.47$, is calculated as $C_{\text{friction}} = 1 + (\gamma - 1) / \sqrt{p_r}$. $\gamma = c_p / c_v = 1.4$ is the ratio of the air specific heat at constant pressure and volume respectively,

$p_r = \eta c_p / \kappa_T = 0.72$ is the Prandtl number and κ_T is the air thermal conductivity.

2.4. Wave propagation properties

As the periodic system under study is invariant under axial translation, the solution in any cell of the structure can be expressed in terms of the solution in any other cells by repeated application of the transmission relation. For an infinite number of resonators, it is described using Block wave theory [9] by the condition $f(x + D) = e^\mu f(x)$, that allows the relation (3) on the pressure amplitudes between two cells to be written as [5]

$$\begin{bmatrix} C_{n+1}^+ & C_{n+1}^- \end{bmatrix}^T = e^\mu \begin{bmatrix} C_n^+ & C_n^- \end{bmatrix}^T, \quad (11)$$

with e^μ the eigenvalue of the transfer matrix \mathbf{T} . The analysis of the characteristic wave solutions is then reduced to the eigen-analysis of \mathbf{T} . The eigenvalue e^μ determines the propagation of a particular wave type defined by its corresponding eigenvector $[v^+ \ v^-]^T$ that contains a linear combination of positive and negative-going plane waves. The solutions μ are complex-valued and composed of a real part, μ_r , the attenuation constant, that describes the attenuation of energy of the travelling waves, and an imaginary part, μ_i , the phase constant, responsible of phase changes through the waves propagation. Frequency ranges occur in which $\mu_r = 0$ and $\mu_r \neq 0$ denoted pass and stop bands, respectively. In the case of a semi-infinite duct, only the positive-going plane wave exists and Eq. (11) can be simplified to

$$\begin{bmatrix} C_n^+ & C_n^- \end{bmatrix}^T = a_n \begin{bmatrix} v_1^+ & v_1^- \end{bmatrix}^T, \quad n = 1, 2, \dots, N. \quad (12)$$

Considering that the solution of the system can be obtained by the periodic application of the transmission relation (3), the complex constant a_n is expressed as $a_n = a_1 \lambda_1^{n-1}$ [5].

3. Sound attenuation by periodic arrays of Helmholtz resonators

Once the analytical model has been established, the results will be verified against other works in the literature. They will also be used as a design tool for predicting the expected attenuation performance and for a proper optimization of the physical parameters considering different cost

functions. In particular, we will focus on the study of two main constitutive parameters such as the effective acoustic path length in the resonators cavity and the axial separation distance between two consecutive resonators in order to maximize the averaged TL in the low frequency range. By default, the HRs used in the simulations have the following nominal parameters: a neck diameter $d_1 = 3.5\text{ cm}$, a neck length $t_1 = 4.55\text{ cm}$ connected to a square cavity of depth $D_1 = 4\text{ cm}$ and of surface area $S_p = 8.33 \times 8.33\text{ cm}^2$. Each HR is plugged onto the top wall of a semi-infinite rigid rectangular duct of cross-sectional area $S_d = 3.63 \times 3.63\text{ cm}^2$ without flow. The HRs are evenly separated by a distance $D = 40\text{ cm}$. For comparison purposes, these parameters are those used in [5] in which a planar wave regime is assumed in the duct, but not in the neck nor in the cavity, leading to a modal formulation for the HR input impedance Z_b . In our case, simulations are conducted up to 1 kHz, well below the first duct, neck and cavity cut-on frequencies, respectively at 4250 Hz, 4857 Hz and 1810 Hz. A plane wave regime has been assumed in all the fluid domains, including at the neck-cavity interface.

3.1. Sound attenuation by HR arrays

Figure 2 compares the averaged TL of an array made up of 5 HRs to that of a single HR assuming for Z_b either Maa's single hole model given by Eq. (2) or Ingard's model, given in Sec. 4.5.3 of [1], for the transfer impedance Z_{p1} of the neck.

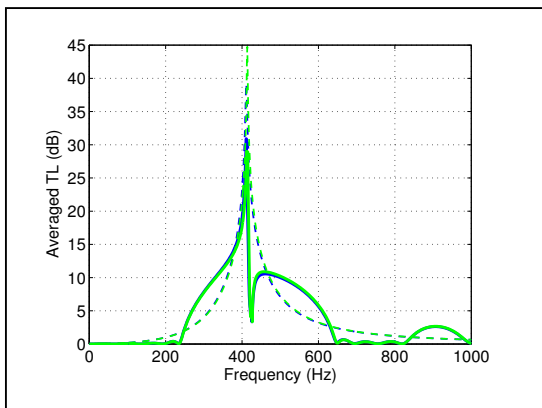


Figure 2. Influence of the input impedance model on the averaged TL of side-branch resonators made up of a single HR (dashed blue: Maa; dashed green: Ingard) and an array of $N_R = 5$ equally spaced HRs (thick blue: Maa; thick green: Ingard).

Figure 2 well compares with Fig. 8 from [5]. It shows that a major feature due to a periodic array of HRs is to provide extra bandwidths over which the sound attenuation is enhanced with respect to that of a single HR that only exhibits a sharp and narrow peak centred around its Helmholtz resonance frequency $f_H = 411\text{ Hz}$. A periodic array of HRs provides an averaged TL greater than that due to a single HR over the bands 248–380 Hz, 465–630 Hz and 843–982 Hz. Above f_H , stop bands appear around the so-called Bragg resonance frequencies, $f_{n,B}$, that occur whenever the separation distance between two resonators comprises an even or odd number of half-wavelengths, *e.g.* when $k_{n,B}D = n\pi$, $n \geq 1$ or equivalently when $f_{n,B} = nc_0/(2D)$. This creates pressure-release local axial resonances between two consecutive neck-duct junctions that block the propagation of sound waves, as observed in Fig. 2 over the bands 425–650 Hz and 820–1000 Hz.

Moreover, both Maa and Ingard models provide very similar averaged TL values whatever the number of resonators, with a Helmholtz resonance frequency predicted by Ingard's model at 414 Hz, slightly above that predicted by Maa's model at 411 Hz. This is due to the added length of the neck correctly estimated by both models at the neck-duct interface, but overestimated at the neck-cavity junction by Maa's model that assumes piston radiation in a baffled aperture. This error decreases when the cavity surface area S_p increases.

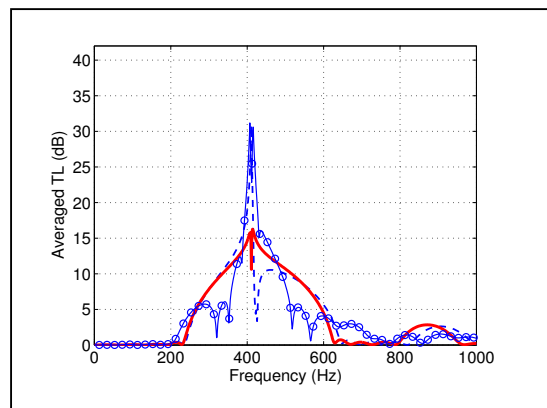


Figure 3. Influence of the spatial period on the averaged TL of an array made up of 5 HRs: $D = 40\text{ cm}$ (dashed blue), $D = D_{\text{opt}} = 42\text{ cm}$ (thick red) and $D = D_{\text{opt}} \pm 2\%$ (thin blue with circles).

Figure 3 shows the influence of structural periodicity on the averaged TL of an array made up of 5 HRs. In accordance with [10], there exists an optimal separation distance D_{opt} between two consecutive resonators that maximizes the bandwidth of the averaged TL around f_H . It is achieved when the Helmholtz frequency coincides with the first Bragg resonance frequency, *e.g.* when $f_H = f_{1,B} = c_0 / (2D_{\text{opt}})$. From Fig. 3, it can be seen that increasing the spatial period between the HRs from $D = 40$ cm to $D_{\text{opt}} = 42$ cm significantly broadens the width of the first stop band, due to merging between the Helmholtz and the first Bragg resonances. Hence, the first stop band now ranges between 230 Hz and 630 Hz, but this is achieved at the expense of a reduction in the averaged TL peak value from 31 dB down to 16 dB. Figure 3 also shows that applying a random perturbation of only 2% standard deviation to the optimal separation distance breaks the coincidence effect, reduces the bandwidth of large attenuation, while it sharpens and increases the averaged TL peak value. Also, the high-order Bragg stop bands do not appear anymore in this case. Hence, optimising the attenuation performance of the HR array appears to require a fine tuning and a low variability of the HRs separation distance.

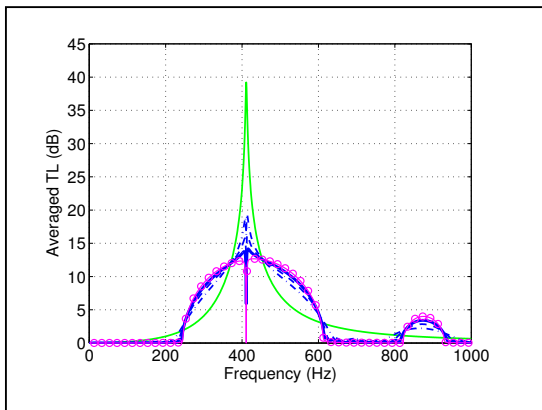


Figure 4. Influence of the number of resonators on the averaged TL of a periodic array of HRs with optimal separation distance: $N_R = 1$ (green), $N_R = 3$ (dash-dotted blue), $N_R = 5$ (dashed blue), $N_R = 10$ (thick blue) and an infinite number of HRs (magenta with circles).

Figure 4 clearly shows that, as the number of resonators increases, the averaged TL of an array with optimal separation distance between the HRs asymptotically tends towards the attenuation

constant, $20 \log_{10}(e^{\mu_r})$, that assumes an infinite number of resonators and which results from an eigen-decomposition of the transfer matrix of the unit cell, as seen in Sec. 2.4. One observes that the asymptotic axial attenuation at the two first stop-bands is already well approximated with 5 resonators, albeit with a TL peak value higher than the asymptotic one. This convergence result is also observed if the HR separation distance is not optimal.

3.2. Sound attenuation by UHR arrays

It has been seen that a single HR with a shallow cavity is efficient to attenuate the propagation of tonal noise in the mid-frequency range. Moreover, it was shown that periodic arrays of HRs exhibit broad stop-band over which the axial attenuation is enhanced. For instance, Fig. 4 shows that the first stop band starts at 230 Hz. Of interest is to shift the stop bands towards lower frequencies while keeping the same cavity depth for the HRs.

This can be achieved by inserting a rectangular coil in the cross-sectional plane of the square cavity, centred on the neck-cavity opening and whose height occupies the whole cavity depth. According to Eq. (8), for a given length (or width) of the cavity, the thickness of the coil walls, their separation distance and the number of folding turns determine a desired acoustic path length in the cavity, and so enable to tune f_H to lower frequencies. Note that $2w$ should stay greater than the neck diameter in order to avoid obstruction of the neck-cavity opening.

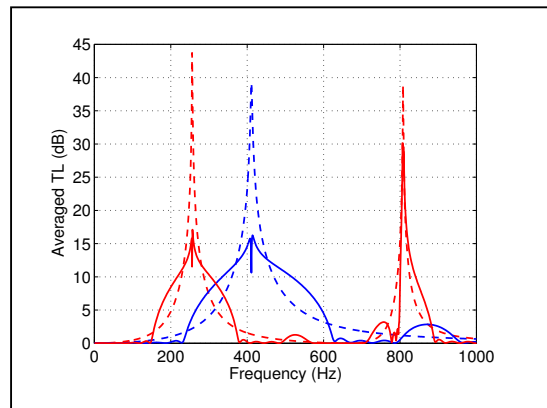


Figure 5. Influence of a coiled cavity on the averaged TL of a single HR (dashed curves) and of a periodic array of 5 HRs (thick curves) considering an air cavity (blue) or a folded rectangular path in the cavity cross-sectional plane (red).

Figure 5 shows that a periodic array of 5 coiled UHRs, with an optimal spatial period $D_{\text{opt},c} = 67\text{cm}$ and $p=2$ turns in each cavity, shifts the Helmholtz resonance frequency from 411 Hz down to $f_{\text{H},c} = 256\text{Hz}$ while achieving broad attenuation bandwidth that extends between 146 Hz and 380 Hz, with a peak attenuation value similar to that of the HR array. This first stop band still results from coincidence between $f_{\text{H},c}$ and $f_{1,B}$. The maximum attenuation is reached for a subwavelength cavity depth of $\lambda_{\text{H},c}/34$ with $\lambda_{\text{H},c}$ the acoustic wavelength at the Helmholtz resonance, but a more characteristic lengthscale to consider should be $D_{1,c}$, the effective acoustic path length in the coiled resonator, which is only $\lambda_{\text{H},c}/5$ at 256 Hz.

At 808 Hz, one observes in Fig. 5 a narrow, but high amplitude attenuation peak. It is the first high-order quarter-wavelength resonance of the HR that, in a first approximation, occurs at $f_{n,1/4,c} = (2n+1)c_0/[4(D_{1,c} + t_1)]$ with $n \geq 1$. It overestimates by 7% for $n=1$ the frequency of maximal attenuation, and by less than 2% the higher-order peaks ($n \geq 2$, not shown). These resonances occur due to the back-cavity cross section of the coiled resonator, $S_{p,c} = 4w^2$, being only slightly greater than the neck cross-section S_1 , so that $S_{p,c}/S_1 \approx 1.7$ for the UHR array whereas $S_p/S_1 \approx 7.6$ for the HR array. Note that $S_{p,c}/S_1$ tends to 1 as the number of turns in the folded resonator increases, *e.g.* when one aims at lowering the UHR Helmholtz resonance frequency. It was found that increasing the number of turns further decreases f_{H} but the bandwidth of the first stop band decreases accordingly, so that, not only the spatial period, but also the UHR constitutive parameters such as d_1 , t_1 and S_p should then be optimized to enhance the attenuation bandwidth.

Figure 6(a) confirms that the amplitude and bandwidths of the attenuation stop-bands achieved by an array of 5 HRs and UHRs are already close to their asymptotic values reached when assuming an infinite number of resonators and obtained from an eigen-analysis of their transfer matrices. It can be seen from Fig. 6(b) that two neighboring cells exhibit phase inversion within the first stop-band, but also within the odd higher-order stop bands whereas in-phase response is observed within the

stop-bands of even orders. Phase inversion due to the Helmholtz resonances at 256 Hz (resp. 411 Hz) for the UHR (resp. HR) arrays can be seen through a narrow gap at these frequencies within the first stop band. If the resonators separation distance was not optimized, the gap would sharply decrease down to zero due to a marked phase inversion at the Helmholtz resonance.

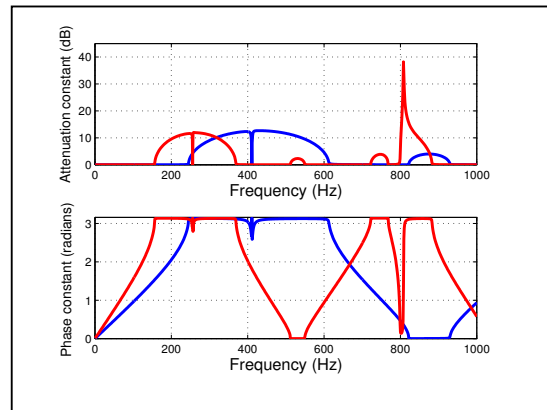


Figure 6. Influence of a coiled cavity on the attenuation constant (a) and on the phase constant (b) of a periodic array of HRs considering an air cavity (blue) or a rectangular coil in the cavity (red).

3.3. Effect of a uniform flow

Figure 7 shows the effect of a low speed uniform grazing flow on the attenuation performance of HR and UHR arrays. Rice's model [11] has been used to describe the input resistance at the neck-duct opening of a Helmholtz resonator under grazing flow conditions. According to what is reported in [1] and [11], grazing flow increases the acoustic specific resistance by a fraction (0.5) of the Mach number. As for the reactance, it is agreed that grazing flow decreases the outer end-correction of the neck length at the neck-duct opening. Cumming's empirical reactance model [12] has been implemented. It provides a reduced end-correction whenever the frequency f is lower than u^*/d_1 with $u^* = 1.8\text{ms}^{-1}$ the friction velocity associated to a low speed Mach number of 0.15 and a turbulent Reynolds number of $8 \cdot 10^4$. It can be seen from Fig. 7 that the resistance added to the HRs and UHRs by the flow decreases by about 10 dB the peaks of averaged TL and slightly increases the widths of the first stop-bands. The flow mass end corrections due to the low flow speed provide minute increases of the Helmholtz resonance frequencies.

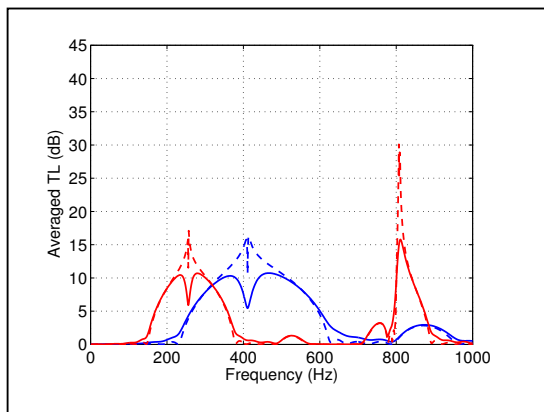


Figure 7. Influence of a uniform flow at Mach 0.15 on the averaged TL of a periodic array of 5 HRs (blue) and UHRs (red) without flow (dashed curves) and with flow (thin curves).

4. Conclusions

An analytical model has been delineated to predict the averaged TL of periodic arrays of HR and UHR side-branch resonators in the flow and no-flow cases. In the no-flow case, Ingard and Maa impedance models for the HRs neck provide similar averaged TL values. A periodic array of HRs provides extra bandwidths due to Bragg resonances and over which the sound attenuation is enhanced with respect to that of a single HR that only exhibits a sharp peak centred around its Helmholtz resonance, here at 361 Hz. Optimizing the spatial period between the HRs at half the Helmholtz resonance wavelength significantly broadens the width of the first stop band, due to merging between the Helmholtz and the first Bragg resonances. But, this advantage is lost by slight perturbations of the HR structural periodicity. They still enable to achieve a trade-off between large bandwidth or high peak level of sound attenuation at the Helmholtz resonance frequency. Coiling up the partition back space significantly downshifts the Helmholtz resonance towards low frequencies, here from 411 Hz to 256 Hz while keeping a constant cavity thickness of 4 cm. Meanwhile, stop- and pass-bands are maintained by the periodic structure of the array. A uniform low-speed flow of Mach lower than 0.15 adds extra resistance to the HR and UHR input impedance, thereby decreasing by about 10 dB the averaged TL peak, with only a slight effect on the reduction of mass-end correction at the HR and UHR openings. In presence of flow, micro-perforated patches should be inserted at the neck-duct openings to avoid pressured drops along the

side-branch resonators and their influence on the averaged TL should be assessed.

Acknowledgements

This work has been funded by The Ministerio de Economía y Competitividad in Spain, project TRA2017-87978-R, “Programa Estatal de Investigación, Desarrollo e Innovación Orientada a los Retos de la Sociedad”, and by the programme A*MIDEX Excellence Initiative of Aix-Marseille University, a French “Investissements d’Avenir” programme, carried out in the framework of the Labex Mechanics and Complexity AAP2.

References

- [1] U. Ingard. *Noise Reduction Analysis*. Jones and Bartlett Publishers, Sudbury, Massachusetts, 2010.
- [2] A. Trochidis, Sound transmission in a duct with an array of lined resonators. *Journal of Vibration and Acoustics* 113 (1991), 245–249.
- [3] C.E. Bradley. Time harmonic acoustic Block wave propagation in periodic waveguides. Part I. Theory. *Journal of the Acoustical Society of America* 96 (1994), 1844–1853.
- [4] N. Sugimoto, T. Horioka. Dispersion characteristics of sound waves in a tunnel with an array of Helmholtz resonators, *Journal of the Acoustical Society of America* 97 (1995), 1446–1459.
- [5] X. Wang, C.M. Mak. Wave propagation in a duct with a periodic Helmholtz resonator array, *Journal of the Acoustical Society of America* 131 (2012), 1172–1182.
- [6] Y. Li, B.M. Assouar. Acoustic metasurface-based perfect absorber with deep subwavelength thickness, *Applied Physics Letters* 108 (2016), 063502.
- [7] D.Y. Maa. Potential of microperforated panel absorber, *Journal of the Acoustical Society of America* 104 (1988), 2861–2866.
- [8] M. Åbom, S. Allam. *Dissipative Silencers Based on Micro-Perforated Plates*, SAE Technical Paper 2013-24-0071, 2013, doi:10.4271/2013-24-0071.
- [9] C. Kittel. *Introduction to Solid State Physics*, 6th ed. Wiley, New York, 1986, Chap. 8.
- [10] C. Cai, C.M. Mak. Noise control zone for a periodic ducted Helmholtz resonator system, *Journal of the Acoustical Society of America* 14 (2016), EL471–477.
- [11] E.J. Rice. A theoretical study of the acoustic impedance of orifices in a presence of a steady grazing flow, NASA Technical Memorandum (1976) TM-X-71903.
- [12] A. Cummings. The effects of grazing turbulent pipe-flow on the impedance of an orifice, *Acta Acustica united with Acustica*, 61 (1986), 233–242.